

# SANDIA REPORT

SAND2008-0679

Unlimited Release

Printed January 2008

## Summary Report: Universal Fuel Processor

James E. Miller, Chad L. Staiger, Christopher J. Cornelius, Steven F. Rice, Eric N. Coker, Constantine A. Stewart, Richard A. Kemp, and Lyle M. Pickett

Prepared by  
Sandia National Laboratories  
Albuquerque, New Mexico 87185 and Livermore, California 94550

Sandia is a multiprogram laboratory operated by Sandia Corporation, a Lockheed Martin Company, for the United States Department of Energy's National Nuclear Security Administration under Contract DE-AC04-94AL85000.

Approved for public release; further dissemination unlimited.

Issued by Sandia National Laboratories, operated for the United States Department of Energy by Sandia Corporation.

**NOTICE:** This report was prepared as an account of work sponsored by an agency of the United States Government. Neither the United States Government, nor any agency thereof, nor any of their employees, nor any of their contractors, subcontractors, or their employees, make any warranty, express or implied, or assume any legal liability or responsibility for the accuracy, completeness, or usefulness of any information, apparatus, product, or process disclosed, or represent that its use would not infringe privately owned rights. Reference herein to any specific commercial product, process, or service by trade name, trademark, manufacturer, or otherwise, does not necessarily constitute or imply its endorsement, recommendation, or favoring by the United States Government, any agency thereof, or any of their contractors or subcontractors. The views and opinions expressed herein do not necessarily state or reflect those of the United States Government, any agency thereof, or any of their contractors.

Printed in the United States of America. This report has been reproduced directly from the best available copy.

Available to DOE and DOE contractors from  
U.S. Department of Energy  
Office of Scientific and Technical Information  
P.O. Box 62  
Oak Ridge, TN 37831

Telephone: (865) 576-8401  
Facsimile: (865) 576-5728  
E-Mail: [reports@adonis.osti.gov](mailto:reports@adonis.osti.gov)  
Online ordering: <http://www.osti.gov/bridge>

Available to the public from  
U.S. Department of Commerce  
National Technical Information Service  
5285 Port Royal Rd.  
Springfield, VA 22161

Telephone: (800) 553-6847  
Facsimile: (703) 605-6900  
E-Mail: [orders@ntis.fedworld.gov](mailto:orders@ntis.fedworld.gov)  
Online order: <http://www.ntis.gov/help/ordermethods.asp?loc=7-4-0#online>



SAND2008-0679  
Unlimited Release  
Printed January 2008

## Summary Report: Universal Fuel Processor

James E. Miller, Chad L. Staiger, Christopher J. Cornelius, \*Steven F. Rice,  
Eric N. Coker, Constantine A. Stewart, Richard A. Kemp, and \*Lyle M. Pickett

Sandia National Laboratories  
P.O. Box 5800  
Albuquerque, NM 87185

\*P.O. Box 969  
Livermore, CA 94551-0969

### Abstract

The United States produces only about 1/3 of the more than 20 million barrels of petroleum that it consumes daily. Oil imports into the country are roughly equivalent to the amount consumed in the transportation sector. Hence the nation in general, and the transportation sector in particular, is vulnerable to supply disruptions and price shocks. The situation is anticipated to worsen as the competition for limited global supplies increases and oil-rich nations become increasingly willing to manipulate the markets for this resource as a means to achieve political ends. The goal of this project was the development and improvement of technologies and the knowledge base necessary to produce and qualify a universal fuel from diverse feedstocks readily available in North America and elsewhere (e.g. petroleum, natural gas, coal, biomass) as a prudent and positive step towards mitigating this vulnerability. Three major focus areas, *feedstock transformation*, *fuel formulation*, and *fuel characterization*, were identified and each was addressed. The specific activities summarized herein were identified in consultation with industry to set the stage for collaboration. Two activities were undertaken in the area of feedstock transformation. The first activity focused on understanding the chemistry and operation of autothermal reforming, with an emphasis on understanding, and therefore preventing, soot formation. The second activity was focused on improving the economics of oxygen production, particularly for smaller operations, by integrating membrane separations with pressure swing adsorption. In the fuel formulation area, the chemistry of converting small molecules readily produced from syngas directly to fuels was examined. Consistent with the advice from industry, this activity avoided working on improving known approaches, giving it an exploratory flavor. Finally, the fuel characterization task focused on providing a direct and quantifiable comparison of diesel fuel and JP-8.



## Table of Contents

<b>1.0 Introduction</b> .....	<b>7</b>
<i>1.1 Motivation</i> .....	7
<i>1.2 Background</i> .....	7
<i>1.3 Project Goal and Structure</i> .....	10
<b>2.0 Feedstock Transformation</b> .....	<b>10</b>
<i>2.1 AutoThermal Reforming</i> .....	10
<i>2.2 Oxygen Generation</i> .....	13
<b>3.0 Fuel Formulation</b> .....	<b>15</b>
<b>4.0 Fuel Characterization</b> .....	<b>19</b>

## List of Figures

Figure 1. Overview of syngas and synfuel technologies. ....	8
Figure 2. Schematic diagram of autothermal reactor. ....	11
Figure 3. Optical attenuation probe for soot formation. A) Optical cell with insulation removed. B) Schematic of cell in operation.....	12
Figure 4. Soot formation as a function of steam:hydrocarbon and hydrocarbon:oxygen ratios at 250 and 500 psi. Soot formation decreases transmittance. ....	12
Figure 5. Effect of (A) steam content on H <sub>2</sub> production (A) and methane:oxygen ratio on conversion and H <sub>2</sub> and CO production (CH <sub>4</sub> flow = 0.8 SLPM).....	13
Figure 6. Schematic diagram of HMPU concept and photograph of assembled unit. ....	14
Figure 7. Front view of HTE system with major components identified.....	18
Figure 8. View of reactor furnace. Inset shows dismantled 8-catalyst rack. Reactant gases pass through fixed bed catalysts in downward direction. ....	18
Figure 9. Front (A) and rear (B) view of reactor effluent analysis train.....	19
Figure 10. Distillation profile of #2 diesel fuel and JP-8. boiling points of pure compounds n-hexadecane (NHD, or cetane) and heptamethyl nonane (HMN) are shown for comparison.....	20
Figure 11. Optically-accessible combustion vessel used to characterize and compare JP-8 and standard #2 diesel fuel.....	20
Figure 12. Illustration of liquid and vapor penetration length within combustion chamber.....	21
Figure 13. Liquid penetration of JP-8 is less than that of #2 diesel fuel but matches that of single component reference fuel heptamethylnonane (HMN)....	21

## **List of Tables**

Table 1. Performance characteristics for individual HMPU components.....	14
Table 2. Oligomerization catalyst preparation and results. ....	16

## 1.0 Introduction

### 1.1 Motivation

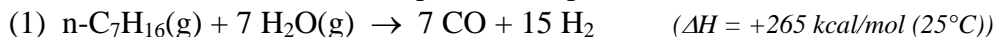
During the decade spanning 1990-2000 energy consumption in the United States increased 17% and in the year 2000 roughly 30% of the nation's total energy consumption was imported. The bulk of energy imported into the country is in the form of petroleum. Currently, the U.S. produces only about 1/3 of the more than 20 million barrels of petroleum that it consumes daily and only about 1/3 of the total is used for something other than transportation. That is, oil imports are roughly equivalent to the amount consumed in the transportation sector. Hence the nation in general, and the transportation sector in particular, is vulnerable to supply disruptions and price shocks. Looking forward, the situation is anticipated to worsen as the economies of countries such as China and India grow and competition for limited global supplies increases. Additionally, "Petroleum-nationalism" has re-emerged in Latin America and elsewhere. In this environment, the development of technologies to produce liquid fuels from diverse non-petroleum feedstocks readily available in North America and elsewhere (e.g. petroleum, natural gas, coal, biomass) is a prudent and positive step.

The U.S. military has already begun to respond to the threat posed by our reliance on oil imports by supporting the development of synthetic (non-petroleum-based) or "manufactured" fuels compatible with their needs. Additionally, the military has recognized that standardizing equipment to operate on a single "universal fuel" applicable to all air, ground, naval, and portable power equipment has significant advantages. These benefits include the simplification of planning and executing military operations due to more efficient storage, transportation, and distribution. A similar case can be made that fuels with broader applicability across the civilian economy are preferable to a larger number of "boutique fuels." Thus, for maximum impact, the liquid fuels produced from any and all feedstocks should be similar enough to one another to be interchangeable for most applications with only minor modification (e.g. blending with small amounts of fuel additives).

### 1.2 Background

Producing a single fuel from diversified feedstocks implies that all feedstocks should pass through a common intermediate. The obvious choice is synthesis gas or syngas, a mixture of  $H_2$  and  $CO$  that can be produced from virtually any hydrocarbon. Figure 1 provides an overview of syngas technologies from feedstock transformation (producing syngas) to fuel (or chemical) formulation. Briefly, carbon-based feedstocks are first mechanically and/or chemically pre-treated to yield a material suitable for processing. A few examples would include removing  $H_2S$  and other undesirable contaminants from natural gas and pulverizing solid feedstocks such as coal. The carbon sources then undergo a *feedstock transformation* process to syngas. Technologies for this transformation include steam reforming (SR), partial oxidation (POX), catalytic partial oxidation (CPOX), autothermal reforming (ATR), and variations on these approaches. Manufacturing syngas can account for up to 60% of the investment in synfuel manufacture.

Steam reforming has been used on a large scale by the petrochemical industry to produce hydrogen for at least 70 years. The process has also been promoted as an alternative to incineration for waste treatment. The chemistry of steam reforming can be simply illustrated by the reactions of n-heptane (as an example of a typical hydrocarbon) and carbon (as a stand-in for coal for example) with superheated steam.



The reaction of steam with organics is highly endothermic and thus the process requires high temperatures to drive the reaction forward. Excess steam helps drive the reaction and also suppresses the formation of the relatively stable carbon and poly- nuclear aromatic byproducts that can form.

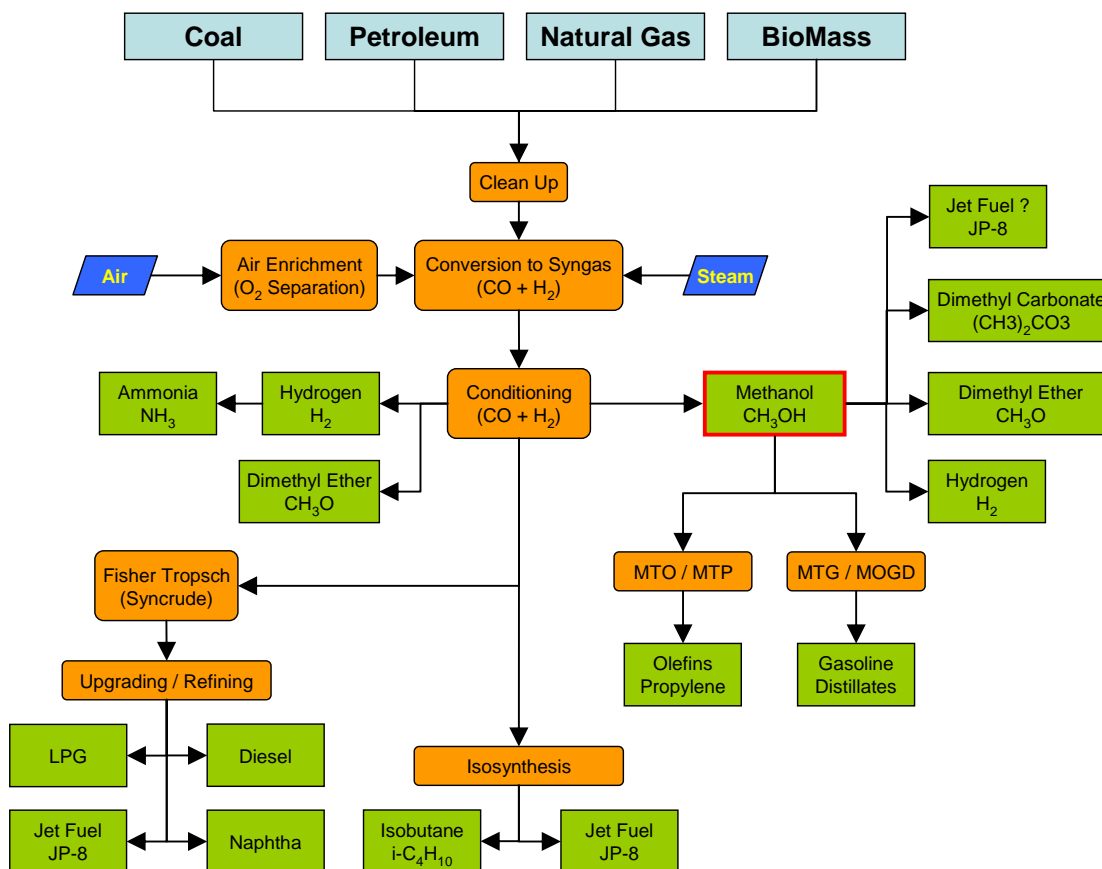
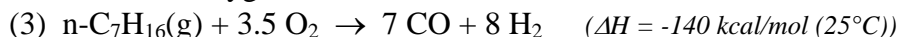


**Figure 1.** Overview of syngas and synfuel technologies.

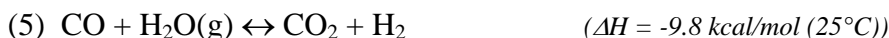
Partial oxidation is essentially an oxygen-starved combustion process. This approach generally requires a source of pure oxygen to avoid the expense and difficulty of carrying a large fraction of N<sub>2</sub> throughout the remainder of the fuel synthesis process. The basic chemistry of partial oxidation can again be illustrated by the reactions of n-heptane and carbon, in this case with oxygen.





As shown, partial oxidation of hydrocarbons is mildly exothermic. Nonselective reactions in partial oxidation can lead to the formation of CO<sub>2</sub>, H<sub>2</sub>O, and more problematically (in gas or vapor phase processes) solid C products known as coke or soot that can plug reactors and other equipment and deactivate catalysts.

Note that the steam reforming reaction produces more H<sub>2</sub> than partial oxidation and that, in the extreme case of a pure carbon feed, steam is required to produce any hydrogen at all. In fact, in syngas processes there is a thermodynamic equilibrium between steam, H<sub>2</sub>, CO and CO<sub>2</sub> that determines the relative amounts of CO and H<sub>2</sub> in the mixture.



The forward reaction as written is exothermic and is known as the water gas shift reaction (WGS). In practice, this reaction allows H<sub>2</sub> to be produced from hydrogen-deficient feedstocks, the reaction being driven by the “burning” of some of the CO to CO<sub>2</sub>. The equilibrium allows the CO to H<sub>2</sub> ratio to be adjusted by manipulating the temperature, and the steam and CO<sub>2</sub> content of the gas stream. A H<sub>2</sub>:CO ratio of about 2 is required for most syngas processes.

Autothermal reforming blends combustion, partial oxidation, and steam reforming so that the exothermic reactions of the carbon source with oxygen balance the endothermic reactions with steam. In essence, the external combustion process required to drive steam reforming is integrated into a reforming reactor. Although the term autothermal reforming is most often applied to reactors processing natural gas or naphtha, gasification reactors that are used to produce syngas from solid products such as coal can also be thought of as a type of autothermal reformers. The energy released by the reaction of oxygen with the solid hydrocarbon drives the volatilization and gasification reactions (reactions 1 and 3, for example) and the subsequent reforming and water gas shift reactions. Some of the advantages of the autothermal approach include feedstock flexibility and the ability to produce syngas with low H<sub>2</sub>:CO ratios.

Steam reforming, particularly steam methane reforming, is the most widely used technology for synthesis gas production. About 20% of the natural gas fed to this process is burned to produce the heat to drive the reforming reaction. Although the process is energy intensive, produces significant quantities of CO<sub>2</sub> and NO<sub>x</sub>, and for natural gas yields a H<sub>2</sub>:CO of about 3 (the ratio is adjusted down by recycling CO<sub>2</sub>), it is economically advantageous for small installations as it does not require an oxygen separation/purification step. The economics of O<sub>2</sub> separation is more favorable for large cryogenic operations. As a result, autothermal reforming (of methane) becomes the economically favorable choice for large facilities, and more generally large facilities are favored when oxygen is required to gasify the feedstock. Still, the cost of oxygen generation can account for up to 40% of the cost of an ATR syngas plant.

The two principal routes for converting syngas to fuel or fuel-like chemicals (*fuel formulation*) are Fischer Tröpsch (FT) synthesis and methanol synthesis (principally the ICI (Syntex) process.) FT and methanol synthesis are mature chemical technologies that have been practiced commercially for decades. The FT approach involves polymerizing the syngas into mid to high molecular weight waxes at elevated pressures over an iron- or

cobalt-based catalyst, and then cracking, isomerizing, and distilling the products into various fuel fractions. As the initial product of FT is linear hydrocarbons, it is particularly suited to the production of diesel, kerosene, and jet fuel type fractions. Isosynthesis is similar to FT, but yields a larger fraction of branched hydrocarbons (particularly i-C<sub>4</sub>); it is not yet useful for directly producing fuels or larger MW compounds. Methanol is commercially prepared from syngas at high pressure over Cu-based catalysts in very high yields. Until recently, the production of the now banned fuel additive MTBE was a major consumer of methanol from syngas. Processes for converting methanol into gasoline-like mixtures, light olefins, ethers, and carbonates have been commercially developed but are not widely practiced.

It has already been demonstrated that jet-fuel (JP-8) can replace diesel fuel used in tanks and other military vehicles. Similarly, it has been demonstrated that synfuels derived from coal can fuel jet engines. Still, some concerns regarding conversion and differences in these fuels and how they impact fuel injection, wear, seals, stability, and other performance issues remain amongst end-users and suppliers. In many cases detailed *fuel characterization* that can alleviate these concerns and provide guidance has been lacking.

### ***1.3 Project Goal and Structure***

The goal of this project was the development and improvement of technologies and the knowledge base necessary to produce and qualify a universal fuel from diverse feedstocks. It was assumed that the market entry point for such technology will be the military, where the necessity of developing alternate hydrocarbon resources and the utility of a logistical fuel for all air, ground, naval, and portable power generation has already been recognized. Jet fuel is the “high consequence” fuel and the proposed universal fuel and thus the effort was targeted towards fuels with properties similar to JP-8. Each of the three major focus areas, *feedstock transformation, fuel formulation, and fuel characterization*, was addressed. Specific activities were identified in consultation with industry to set the stage for collaboration. Two activities were undertaken in the area of feedstock transformation. The first activity focused on understanding the chemistry and operation of autothermal reforming, with an emphasis on understanding, and therefore preventing, soot formation. The second activity was focused on improving the economics of oxygen production, particularly for smaller operations, by integrating membrane separations with pressure swing adsorption. In the fuel formulation area, the chemistry of converting small molecules readily produced from syngas directly to fuels was examined. Consistent with the advice from industry, this activity avoided working on improving known approaches, giving it an exploratory flavor. Finally, the fuel characterization task focused on providing a direct and quantifiable comparison of diesel fuel and JP-8.

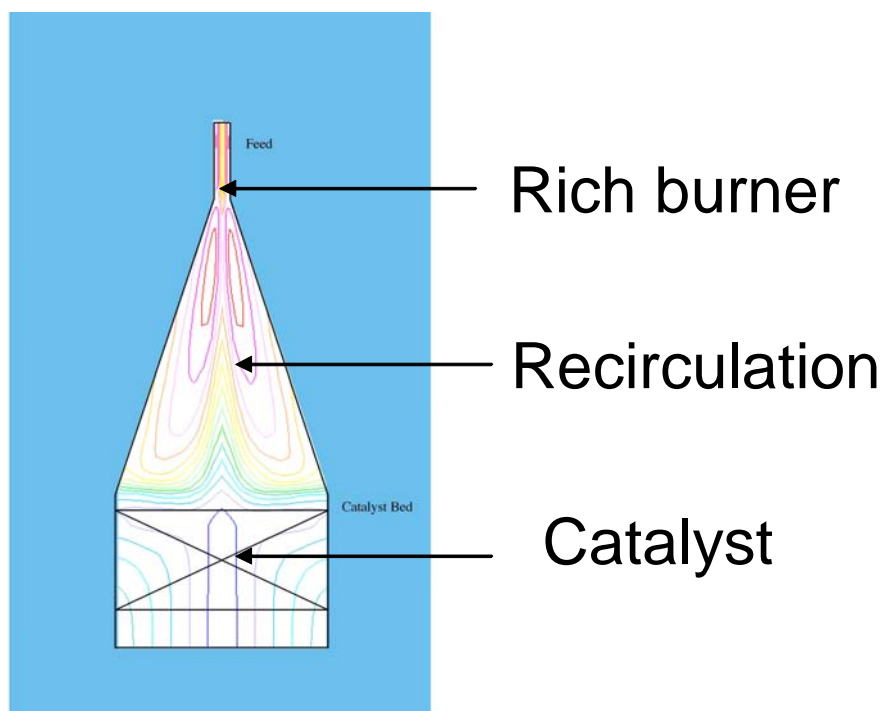
## **2.0 Feedstock Transformation**

### ***2.1 AutoThermal Reforming***

Autothermal reforming of natural gas yields a syngas with a high (>2) H<sub>2</sub>/CO ratio. This can be adjusted down to a more desirable level by directly adding carbon dioxide to the gas feed while simultaneously reducing the steam content. However, the limited experience in plants employing this approach has shown that these conditions may lead to

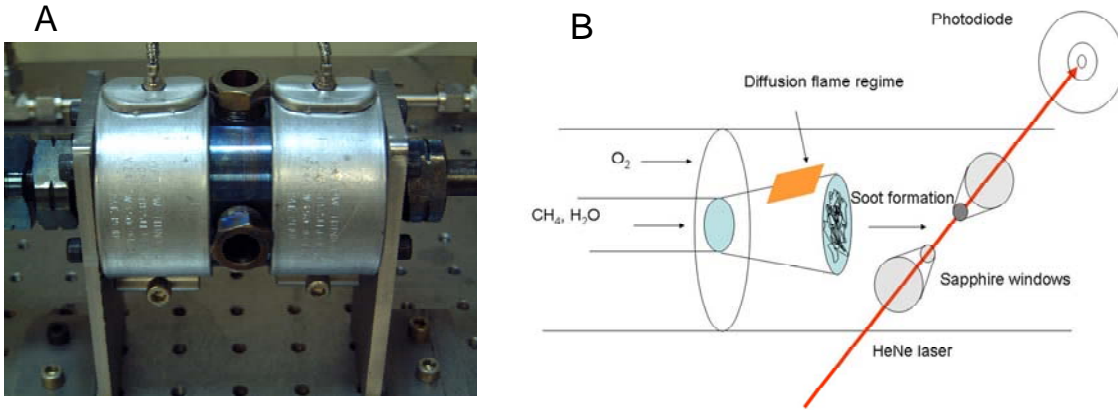
the formation of soot to a degree that can adversely affect the overall unit operation. This technical effort focused on determining the optimum conditions for producing syngas with H<sub>2</sub>/CO ratios needed for high conversion efficiency to liquids while avoiding the production of soot.

Figure 2 shows a simplified schematic of a commercial ATR. Downstream of the burner that provides the heat to drive the chemistry there is a gas recirculation zone followed by the catalyst bed where the reforming reactions occur. The environment in the burner is that of a high-pressure rich diffusion flame. Typical ATRs operate around 300 psi. Although reforming is not favored by high pressure, there are significant downstream processing advantages to be had by operating at an even greater pressure. Soot formation in ATRs is connected to both the burner temperature and flame stoichiometry at the inlet as well as the time/temperature characteristics of the recirculation zone generated by the catalyst bed. In addition, soot precursors can serve to form coke in the catalyst zone.



**Figure 2.** Schematic diagram of autothermal reactor.

A high pressure (1100 psi, maximum) annular laminar flow burner was used to explore the characteristics of soot formation in rich flames similar to those present within an autothermal reformer. Reacting flows consisted of fuel (methane or natural gas), oxidizer (O<sub>2</sub>), steam, and CO<sub>2</sub> in varying ratios. The burner was configured so that fuel and steam composed the inner flow and oxygen the outer flow. A simple optical attenuation probe was used to monitor particulate formation (Figure 3) while the composition of the effluent gases was monitored by gas chromatography.



**Figure 3.** Optical attenuation probe for soot formation. A) Optical cell with insulation removed. B) Schematic of cell in operation.

Experiments were conducted at 250 and 500 psi while varying steam:hydrocarbon (methane and natural gas) and hydrocarbon:oxygen ratios. Typical results are shown in Figure 4. For typical rich flames (2:1 CH<sub>4</sub>/O<sub>2</sub>, black squares) no soot is formed at 250 psi with a modest amount of steam (H<sub>2</sub>O/CH<sub>4</sub> ≥ 0.75). If the steam content is reduced to 0.5 these flames will produce particulates. Leaner flames (1.6:1 CH<sub>4</sub>/O<sub>2</sub>, blue and red triangles) produce few particulates even when H<sub>2</sub>O/CH<sub>4</sub> = 0.25. Natural gas and methane yield similar results. Even under very rich conditions O<sub>2</sub> is not fully consumed. Higher pressure (500 psi, green diamonds) promotes soot formation at equivalence ratios where little soot is formed at 250 psi; steam has little effect, even at H<sub>2</sub>O/CH<sub>4</sub> of 2.0.

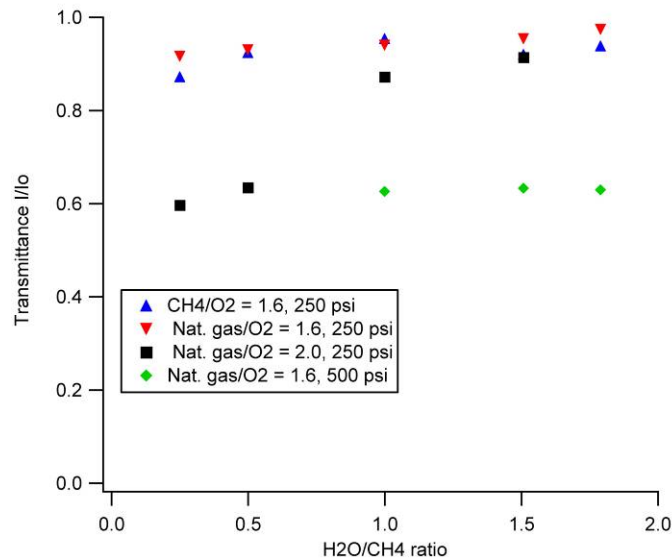


**Figure 4.** Soot formation as a function of steam:hydrocarbon and hydrocarbon:oxygen ratios at 250 and 500 psi. Soot formation decreases transmittance.

H<sub>2</sub> production is sensitive to many parameters including flow velocity, oxidation stoichiometry, steam content, and mixing configuration. Figure 5A shows that decreasing the steam fraction decreases conversion (H<sub>2</sub> production). However, too much

steam can lead to flame extinction (not shown). Figure 5B shows that there is an optimal equivalence ratio for CO/H<sub>2</sub> production at CH<sub>4</sub>:O<sub>2</sub> = 1.6 (0.5 SLPM O<sub>2</sub> in Figure 5B). At CH<sub>4</sub>:O<sub>2</sub> = 1.0 (0.8 SLPM O<sub>2</sub>) combustion chemistry to H<sub>2</sub>O and CO<sub>2</sub> reduce H<sub>2</sub> production. At lower equivalence ratios, conversion is decreased. Results for adding CO<sub>2</sub> in the flame (not shown) suggest that a higher CO/H<sub>2</sub> product is obtained with only a limited effect on soot formation. Calculations indicate that CO<sub>2</sub> participates in reactions in the burner itself.

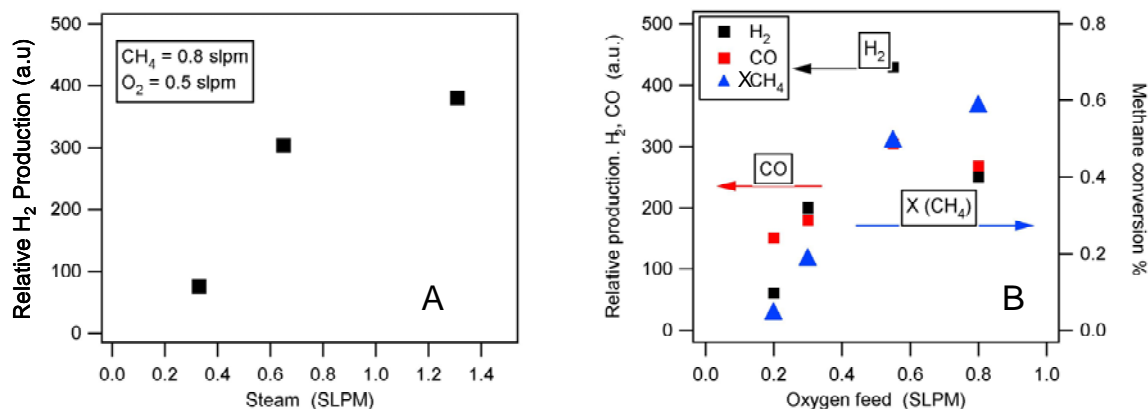


**Figure 5.** Effect of (A) steam content on H<sub>2</sub> production and (B) methane:oxygen ratio on methane conversion and H<sub>2</sub> and CO production (CH<sub>4</sub> flow = 0.8 SLPM).

The stages of soot formation include precursor formation, polycyclic aromatic (PAH) formation, aggregation of PAHs to particulates, and reoxidation of soot particles. In our modeling work, simple elementary reaction modeling calculations for a premixed flow system examined the formation of soot precursors such as benzene and naphthalene. The calculations were performed using the Chemkin 4.0 suite of programs assuming a premixed feed preheated uniformly to 550 °C, applying the most current mechanism of J.A. Miller and co-workers, and assuming adiabatic conditions (flame temperatures = 1300-1600 °C). Admittedly, examining the production of precursors does not encompass the entire soot production process; and furthermore, an annular burner is not the same as a premixed burner. However, the calculations clearly indicate that oxidation stoichiometry is the dominant parameter in determining the degree to which these precursors are formed and that steam, pressure, and CO<sub>2</sub> are less important. The results from the experiments agree in that when the CH<sub>4</sub>:O<sub>2</sub> ratio is much less than 2, soot is not formed. However, the calculations generally do not capture the important role of steam.

## 2.2 Oxygen Generation

Current membrane processes that enrich air only achieve oxygen streams with 35 to 40 mol% on a single pass. Higher oxygen contents are typically realized through pressure swing adsorption (PSA) and cryogenic distillation techniques. These methods can produce 95 to >99 mol% oxygen streams. However, PSA units only recover 30-45% of the oxygen from air and hence energy utilization is poor. The Hybrid Membrane-PSA unit (HMPU) that consists of a membrane system upstream of a PSA system was conceived as a way to improve this situation. In this HMPU concept, an upstream membrane first removes water, argon, and a fraction of the nitrogen, allowing the PSA

bed size to be reduced by almost 60% and possibly more with system optimization. It was anticipated that the hybrid system design would result in an overall system that is smaller and more energy efficient unit and that would have air recovery efficiencies approaching an unprecedented 75%.

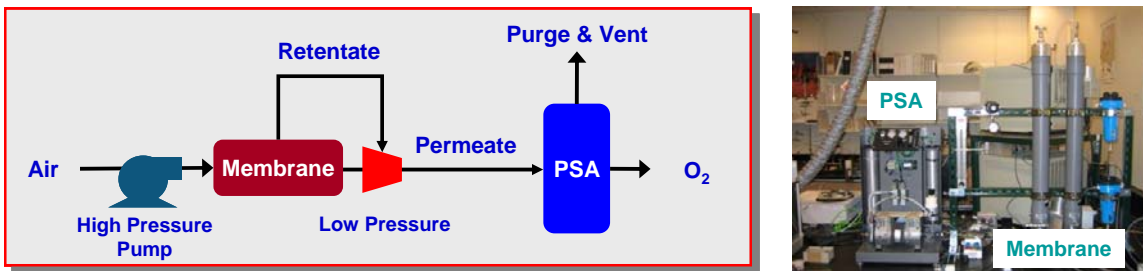


**Figure 6.** Schematic diagram of HMPU concept and photograph of assembled unit.

The design for the HMPU consists of four components (Figure 6); a high pressure pump, membrane module, gas booster and a pressure swing adsorption (PSA) unit. To demonstrate and evaluate the concept, components were purchased and assembled. The measured performance characteristics for the individual components of the HMPU are shown in Table 1. Gas chromatography and a high resolution oxygen sensor (Sable Systems, Inc) were used to identify the components of the gas mixtures exiting the membrane and PSA. Both the membrane module and PSA outputs prior to HMPU construction are consistent with mass balance calculations. Unfortunately, argon concentrations could not be fully resolved.

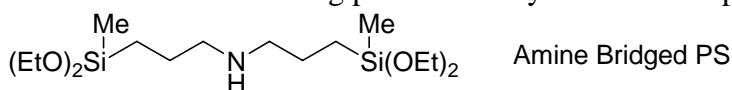
**Table 1.** Performance characteristics for individual HMPU components.

	<b>Membrane</b>	<b>PSA</b>
<b>Manufacturer</b>	Air Products Model PA3030-P1-PA-00	OGSI Model OG-15
<b>Input</b>	Air (70 L/min @ 83 psig)	Air (125 L/min @ 30 psig)
<b>Oxygen Rich Output</b>	39% O <sub>2</sub> + Ar 61% N <sub>2</sub> (38 L/min @ 2 psig)	99% O <sub>2</sub> + Ar 1% N <sub>2</sub> (5 L/min @ 9 psig)
<b>Membrane Retentate</b>	8% O <sub>2</sub> + Ar 92% N <sub>2</sub> (34 L/min @ 80 psig)	

The HMPU was assembled using building supplied compressed air in lieu of an air compressor. A booster pump/pressure recovery device between the membrane and PSA unit was not used. The feed requirements for the PSA in its “off the shelf” configuration are 125 L/min, however a combination of two membrane modules only delivered 83 L/min of enriched oxygen. A third membrane module was added and the pressure input of the membrane module was increased to 100 psig to get the required 125 L/min flow rate for the PSA system to operate correctly. The oxygen output of this highly unoptimized system was 98.0 to 98.2 % at 5 L/min and 9 psig. Potentially the purity of oxygen could be increased to 99%+ by recycling the purge/vent stream of the PSA into

the membrane input, however this was not investigated. A technical advance for the HMPU was submitted (SD# 10351).

Higher oxygen selectivity over nitrogen and argon would lead to a smaller oxygen generation system. Bridged polysilsesquioxane (PSSQ) and polysiloxane (PS) materials were investigated for use as highly oxygen selective membrane materials to potentially replace the materials found in the membrane modules currently being used in the HMPU. Conditions were optimized for coating tubular alumina supports. Tubular supports allow for a higher ratio of membrane area to module volume compared to flat membranes. A two-step coating process was employed to minimize membrane defects. The tubular alumina support was initially dip coated and calcined with a layer of surfactant templated silica (base coat). The coating procedure for the base coat has been previously optimized by Brinker *et al.* A top coat containing the O<sub>2</sub> selective PSSQ or PS material was applied by dip coating and subsequent heat treatment. Initial attempts to coat amine bridged PSSQ and PS materials led to Knudsen gas flow, whereby the gas permeability is proportional to the inverse square root of the gases molecular weight. Knudsen flow indicates defects are present in the membrane material. It was believed defects were present at the tube ends and that a sealing procedure may alleviate this problem.



Subsequent studies showed that using a high quality alumina support was essential for uniform PSSQ and PS coatings. In addition, a second PSSQ or PS coating was needed to seal defects on the initial coating laid down on the alumina support. The amine bridged PSSQ materials had oxygen/nitrogen selectivities ranging from 2.3 to 3.8 depending on the coating conditions. The commercial membrane material used in the HMPU only has an oxygen/nitrogen selectivity of 2.1.

### 3.0 Fuel Formulation

This task initially focused on the conversion of small molecules readily produced from syngas into fuel-range molecules, e.g. oligomerization of ethylene. A concerted effort was made to avoid duplication of, or competition with, industrial research. Thus, after consultation with industry, syngas chemistry *per se*, and related technologies such as methanol to gasoline and methanol to olefins were specifically ruled out. As the project progressed it was determined that the most appropriate “pre-competitive” chemistry to pursue was the conversion of CO<sub>2</sub> into an energetic hydrocarbon, e.g. hydrogenation of CO<sub>2</sub> into methanol. Methanol is of interest as a “*primary building block*” that can be converted to secondary chemical building blocks such as light olefins, and fuels or potential fuel additives such as dimethyl ether (DME), or dimethylcarbonate (DMC).

Consistent with the initial focus on the conversion of basic building blocks into diesel-like molecules, we began our studies by concentrating on Cr- and Fe-based catalysts to promote the formation of C-C linkages between small molecules (C<sub>2</sub> to C<sub>4</sub>) to form larger subunits consistent with JP-8 range molecules (C<sub>10</sub> to C<sub>20</sub>). Catalysts were prepared by

treating a zeolite or a mesoporous silica with a transition metal nitrate solution. Metal incorporation was achieved via ion exchange, impregnation, or framework substitution, (Table 2). The catalysts were all dried in air at 130°C, and were then calcined in air at 500°C for 5 hours with a ramp rate of 5°C min<sup>-1</sup> prior to evaluation of their catalytic activity. The small pore ZSM-5 zeolite (pore size ~0.55nm) was chosen based on reports in the literature, while the larger pore Zeolite-Y (0.74nm) as well as a mesoporous silica (5.4nm) were used for comparison.

**Table 2.** Oligomerization catalyst preparation and results.

	Material	Prod. #, description	Metal	Preparation	Max. conv. (%) <sup>†</sup>	Temp for max conv. (°C)
1	ZSM-5-(NH <sub>4</sub> <sup>+</sup> )	Zeolyst CBV55246 Si/Al = 50/1	Cr <sup>3+</sup>	Ion exchange	20	350
2	ZSM-5-(NH <sub>4</sub> <sup>+</sup> )	"	Cr <sup>3+</sup>	Framework substitution	25	350
3	ZSM-5-(NH <sub>4</sub> <sup>+</sup> )	"	Fe <sup>3+</sup>	Ion exchange	8	450
4	Mesoporous Silica	ENC1-10B P.V. = 1.1mL/g	Cr <sup>3+</sup>	Impregnation	<1	N/A

<sup>†</sup> Calculated through reduction in ethylene concentration relative to feed as monitored by on-line micro-GC using a 4m poroplot Q column.

The catalysts were evaluated as powders for the oligomerization of ethylene in an atmospheric pressure fixed bed flow reactor. During startup, the catalysts were purged with dry UHP nitrogen while being heated to 150°C. A feed of between 10 and 20 vol.-% ethylene in nitrogen was then passed over the catalyst, and the reactor effluent analyzed by on-line micro-GC, as well as by an off-line GC-MS. The reactor temperature was ramped from 150°C to 450 or 500°C while continuously monitoring gas composition. A reactor bypass line allowed the feed gas composition to be monitored before, during, and after catalyst evaluation. Total gas flow rates were kept at 100 sccm for all tests.

All chromium-based zeolitic catalysts produce about a dozen different ethylene oligomers under the conditions tested. Small amounts of oligomers were already detected at 150 °C, and catalyst activity peaked at 350 – 400 °C (maximum ethylene conversion ~25%). The ion exchanged Cr catalyst also produced aromatic compounds. Because the reactions were run at only atmospheric pressure and with diluted ethylene, high conversions should not be expected, and were not achieved. However, operating under conditions of low conversion allows differences in intrinsic activity of catalysts to be readily identified. The Cr-modified mesoporous silica with pore size ~ 3 nm deactivated rapidly from coking and showed negligible oligomerization, highlighting the importance of shape/size selectivities in the microporous zeolite catalysts with pore sizes < 1 nm. Fe-modified zeolites were less active, showing a maximum ethylene conversion of 8% at 450 °C. After evaluation, all catalysts were dark in color (grey to black), indicating the build up of some carbonaceous deposits, and in most cases a slow drop in activity was seen on holding the catalyst at 450°C. The drop in activity above 400 °C is attributed to catalyst



coking; however, on cooling the catalyst back to 350 °C, some recovery of activity was observed.

Ethylene oligomerization produces only linear hydrocarbons. For fuel applications, branching is desirable. Syngas may be converted into iso-C4s through the isosynthesis reaction, and it is possible that these could be introduced into an oligomerization reaction to produce a branched product. There is precedent in the literature for the activation of iso-butane by H-zeolite in the presence of an olefin at 25°C using a high-pressure fixed bed reactor system [M. Guisnet, N.S. Gnep, *Appl. Catal. A: General*, **146**, 33-64 (1996)]. We attempted to capitalize on this approach, albeit using a batch reactor system at lower pressure. In a batch reactor H-zeolite catalysts (H-Beta and H-Mordenite) oligomerize propylene and iso-butane under mild conditions (50 – 84 °C @ 150 – 320 psig). The products were identified as C6, C9, C12 and C15 oligomers with the majority at C9 and C12. The overall yield was low for this process. Under the same conditions the H-zeolite catalyst with only propylene produced only traces of C6 and C9 oligomers. Only in some isolated cases were the activation of iso-butane and subsequent reaction believed to have occurred; the dominating reaction appears to have been the oligomerization of propylene under the conditions achievable in the current batch reactor system. Modification of the H-zeolites with gallium was investigated in order to influence the product yield, but with only limited success under the conditions of the batch reactor tests.

It was at this point that the task was redirected towards the more pre-competitive topic of CO<sub>2</sub> activation and conversion into fuels. Towards this end, the first and major effort was directed towards refurbishing and recommissioning of two second-hand High Throughput Experimentation (HTE) reactor systems for catalyst evaluation. The first system consists of nine individual 30 cm<sup>3</sup> stirred stainless steel batch reactors capable of being operated at temperatures up to 350 °C and pressures up to 2000 psig. The system is equipped with PID temperature control, real-time temperature and pressure monitoring and trending and logging, and reaction time and temperature ramp control. The second system is a 16-channel fixed catalyst bed reactor unit. The system can be operated over a range of pressures (ambient to 600 psi), temperatures (ambient to 500 °C), and flow rates (ca. 5 – 200 ml min<sup>-1</sup> (@s.t.p.) per channel). Up to 4 process gases (and mixtures thereof) can be passed through the catalyst beds, each gas independently controlled via mass flow controller. Overall system operating pressure can be adjusted by a downstream N<sub>2</sub> buffer. Exhaust gases are vented to a nearby fume hood. Troubleshooting prior to successful operation involved repairs to or replacement of several valves and other gas-handling components, electronics, and computer-interface. Pipework downstream of reactors was in poor condition, requiring extensive cleaning/decontamination, leak detection/correction, and replacement of filters and controlled-flow orifices. The system capability was expanded by integrating a micro-GC with automated reactor channel switching and data logging. Major components of the system are identified in Figures 7,8, and 9.

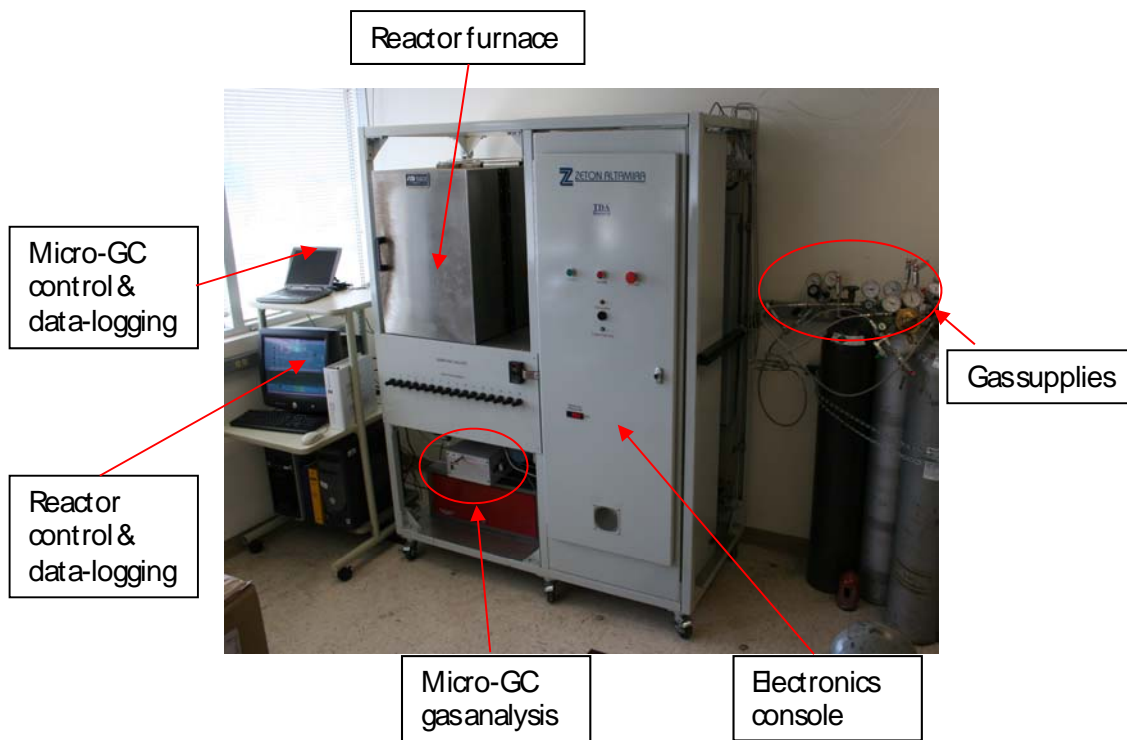


**Figure 7.** Front view of HTE system with major components identified.

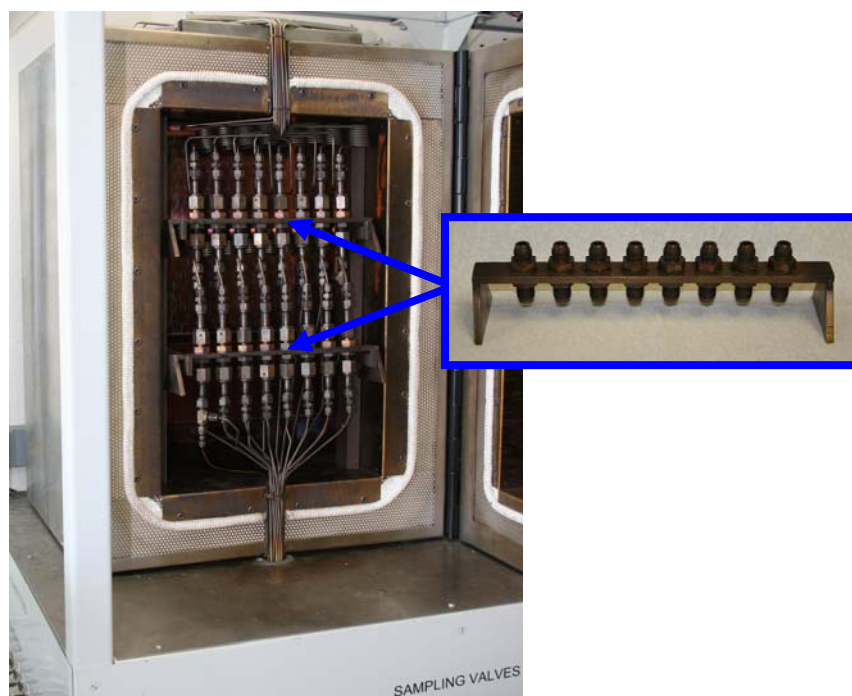


**Figure 8.** View of reactor furnace. Inset shows dismantled 8-catalyst rack. Reactant gases pass through fixed bed catalysts in downward direction.

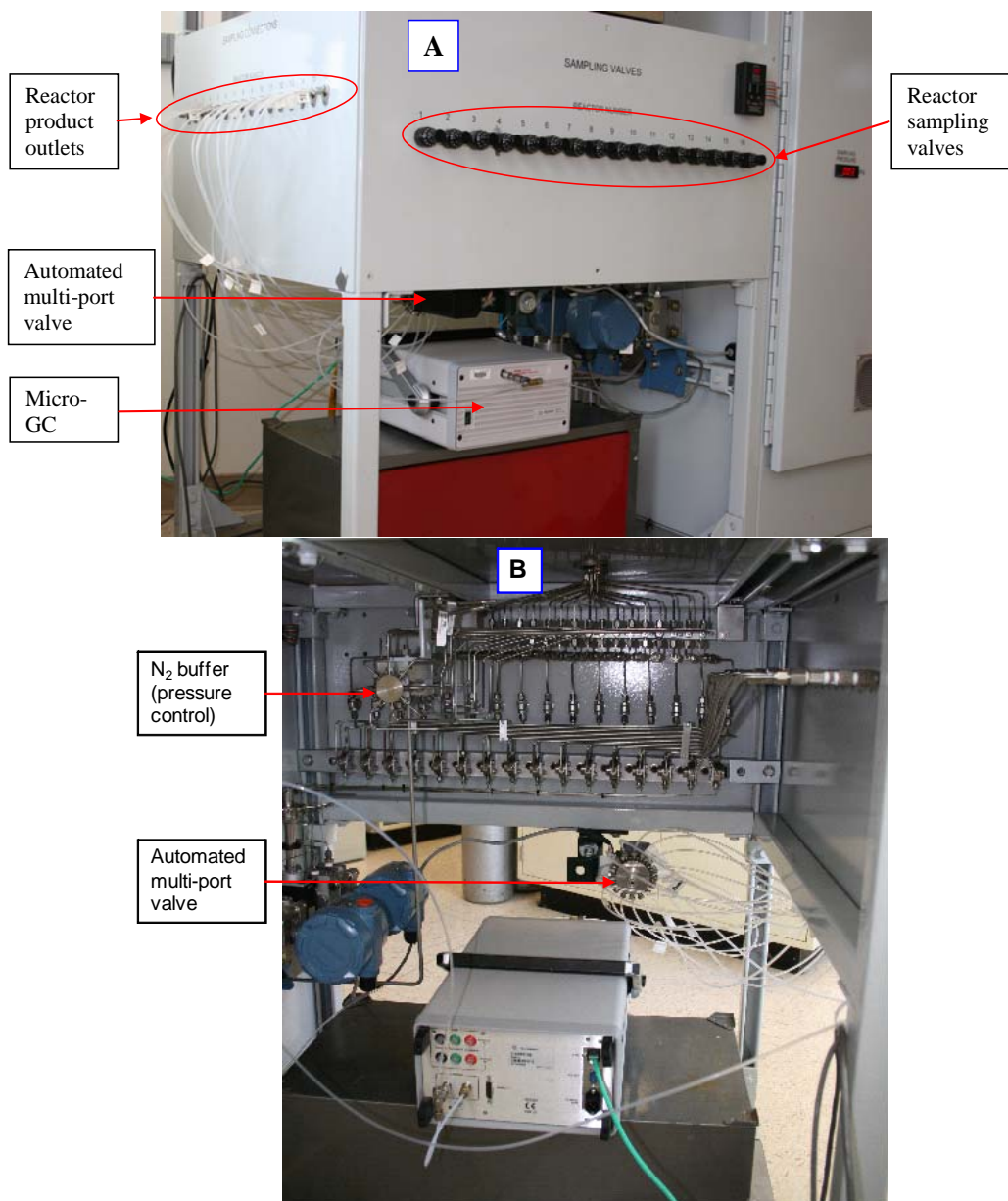


**Figure 9.** Front (A) and rear (B) view of reactor effluent analysis train.

More than 40 catalysts have been prepared as candidates for the  $\text{CO}_2 + \text{H}_2 \rightarrow \text{CH}_3\text{OH}$  reaction and testing has begun. The results are being shared with collaborators who are modeling this and similar reactions and will be presented in future publications.

#### 4.0 Fuel Characterization

This effort focused on characterizing the combustion of JP-8 when used in diesel fuel injectors. The lower-boiling-point range of JP-8, compared to #2 diesel (Figure 10), may lead to more intense heat release because of a higher rate of evaporation from liquid fuel to a combustible vapor. Higher heat-release rates, in turn, can lead to engine damage, as has been reported for military diesel engines fueled by JP-8.

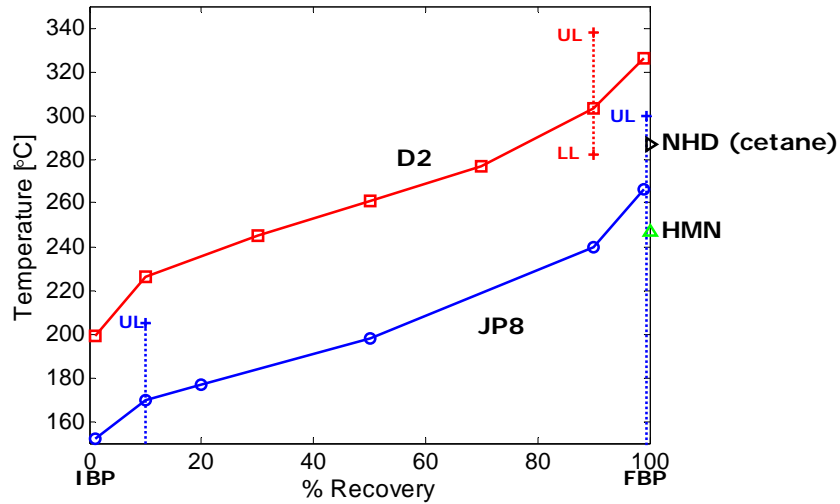
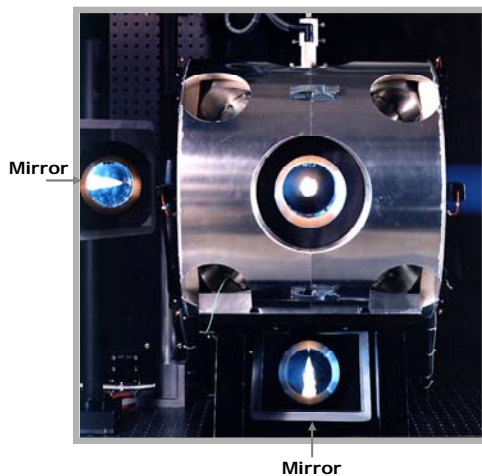


**Figure 10.** Distillation profile of #2 diesel fuel and JP-8. Boiling points of pure compounds n-hexadecane (NHD, or cetane) and heptamethyl nonane (HMN) are shown for comparison.

An optically-accessible combustion vessel (Figure 11) with conditions simulating those of a diesel engine was used to measure liquid and vapor penetration. Liquid spray penetration was measured using laser elastic scatter from fuel droplets. Spray liquid penetration decreases with increasing temperature and reaches a steady-state “liquid length” during injection (Figure 12). The fuel jet vapor boundary was measured using shadowgraph photography. Jet vapor boundary penetration changes little with ambient temperature. There is slightly less vapor penetration at high temperature because of evaporative cooling (contraction) of the jet.



Chamber	Injector
0-21% Oxygen	d = 50-500 mm
700–1300 K	$\Delta P_{inj} = 400-2000$ bar
$3-60 \text{ kg/m}^3 (>200 \text{ bar})$	

**Figure 11.** Optically-accessible combustion vessel used to characterize and compare JP-8 and standard #2 diesel fuel.

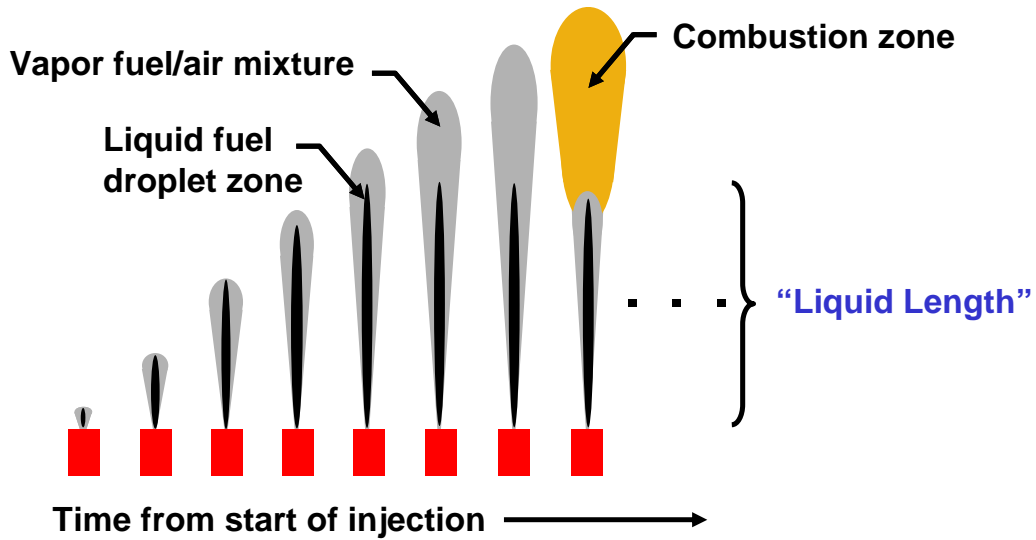


**Figure 12.** Illustration of liquid (black) and vapor (gray) penetration within combustion chamber.

Our study has shown significant differences in the combustion of JP-8 as compared to standard #2 diesel fuel. These differences include: (1) faster evaporation and shorter liquid spray penetration (Figure 13), (2) longer ignition delays, and (3) faster heat-release rates at the time of ignition for JP-8. These tests are the first of their kind for JP-8 and the findings have generated considerable outside interest for future combustion characterization of JP-8-like fuels.

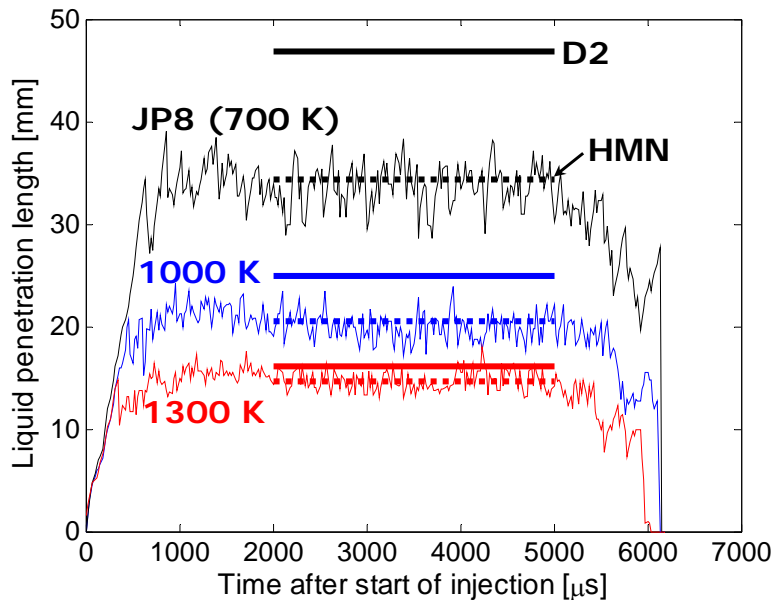


**Figure 13.** Liquid penetration of JP-8 is less than that of #2 diesel fuel (D2, solid lines) but matches that of single component reference fuel heptamethylnonane (HMN, dotted line). Colors indicate temperature: black - 700K, blue - 1000K, and red - 1300K.

**DISTRIBUTION:**

- 5 MS 1349 James Miller, 1815
- 1 MS 1349 Lindsey Evans, 1815
- 1 MS 1349 Eric Coker, 1815
- 1 MS 1349 Rick Kemp, 1815
- 1 MS 1349 Connie Stewart, 1815
- 1 MS 1349 Bill Hammetter, 1815
- 1 MS 1110 Jeff Nelson, 6337
- 1 MS 0734 Ellen Stechel, 6338
- 1 MS 0734 Chad Staiger, 6338
- 1 MS 0734 Chris Cornelius, 6338
- 1 MS 9035 Steve Rice, 8239
- 1 MS 8362 Lyle Pickett, 8362
- 1 MS 0123 LDRD, Donna Chavez, 1011 (electronic only)
  
- 1 MS 0899 Technical Library, 9536 (electronic copy)

